

An hexagonal array of fourfold interconnected hexagonal nodules for modeling auxetic microporous polymers: a comparison of 2D and 3D models

Teik-Cheng Lim · Rajendra Acharya U

Received: 13 March 2009 / Accepted: 1 June 2009 / Published online: 14 June 2009
© Springer Science+Business Media, LLC 2009

Materials and structures that exhibit negative Poisson's ratios are categorized under auxetic systems. Auxetic materials attract considerable attention due to their counter intuitive properties, and such materials have been examined at length by Lakes and co-authors [1, 2], Evans and co-authors [3, 4] and others (e.g., [5–9]). It was shown that a Poisson's ratio as low as $\nu = -12$ was achievable for a polymeric microporous material that consists of nodules interconnected by fibrils [3, 4]. Using rectangular blocks with fibril connections, as shown in Fig. 1a, Alderson and Evans [10, 11] developed 2D models of Young's moduli and Poisson's ratios for varying geometrical parameters and fibril stiffness. The influence of processing parameters on the microstructures, and hence the mechanical properties, of these fibril-linked nodules were experimentally investigated by Alderson et al. [12, 13]. In spite of its rectangular shape selected for the nodules, they were arranged in hexagonal arrangement [10–13]. Recently an interlocking hexagonal model, as depicted in Fig. 1b, was proposed by Ravirala et al. [14]. It is appreciated that the

rectangular models by Alderson and Evans [10, 11] reflect fourfold connectivity, whereas the hexagonal model by Ravirala et al. [14] reflect sixfold connectivity. In this article an attempt is made to develop a Poisson's ratio model using hexagonal nodules with fourfold connectivity. Masters and Evans [15] explored the difference in deformation mechanisms, which is a key difference between the models by Alderson and Evans [10, 11] and Ravirala et al. [14]. This model is hexagonal in both senses—hexagonally shaped blocks in hexagonal array. In this article we take geometrical elements from both models—fibrils from Alderson et al. [10–13] and hexagonal nodules from Ravirala et al. [14]—as shown in Fig. 1c. In the first instance, a 2D model is developed to relate the in-plane Poisson's ratios with the density packing factor of the hexagonal cross-sectioned prisms under a set of conditions. Then, a 3D model is proposed by inference to the cuboid and spherical models. For both cases, only infinitesimally small strains are considered.

The analysis is based on the following conditions: (i) the angle formed by the three mutually neighboring hexagons is 60° , (ii) the ratio of fibril length l to the hexagonal side S depends on the density packing factor, and (iii) the fibril rotates as a rigid rod without taking up volume. The angle 60° specified in condition (i) is valid for infinitesimal deformation considered herein. The geometries are laid out in Fig. 2. Perusal to Fig. 2c shows that the length OC resolved in the X- and Y-directions are

$$\begin{Bmatrix} (\overline{OC})_X \\ (\overline{OC})_Y \end{Bmatrix} = \begin{bmatrix} \sqrt{3} & -\cos \theta \\ 1 & +\sin \theta \end{bmatrix} \begin{Bmatrix} S \\ l \end{Bmatrix}. \quad (1)$$

The angle θ ranges from a minimum of 30° when the density packing factor is 1, to a maximum of 120° when the density packing factor is 0. We herein define the density packing

T.-C. Lim (✉)
School of Science and Technology, SIM University, Clementi Road, Singapore, Singapore
e-mail: alan_tc_lim@yahoo.com

Rajendra Acharya U
School of Engineering, Ngee Ann Polytechnic, Clementi Road, Singapore, Singapore

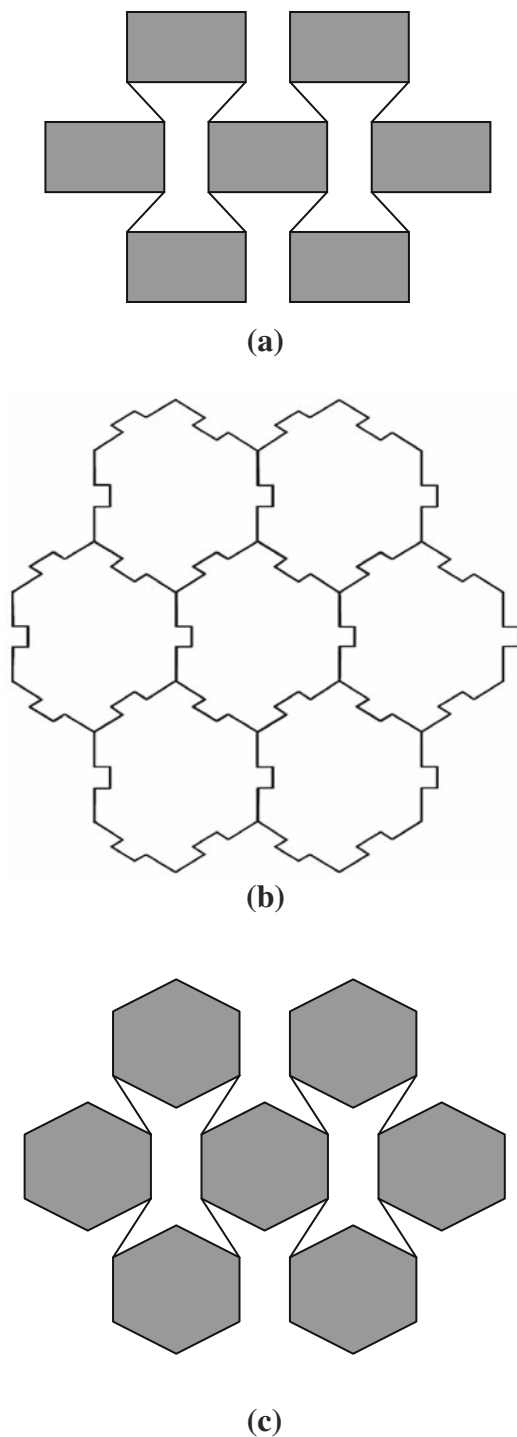


Fig. 1 **a** Nodule-fibril with rectangular blocks in hexagonal arrangement, **b** interlocking hexagons in hexagonal arrangement, **c** nodule-fibril with hexagonal blocks in hexagonal arrangement

factor as the volume fraction that is filled up by nodes such that it ranges from 0 to 1. Based on this definition, the 2D density packing factor is calculated from the area enclosed

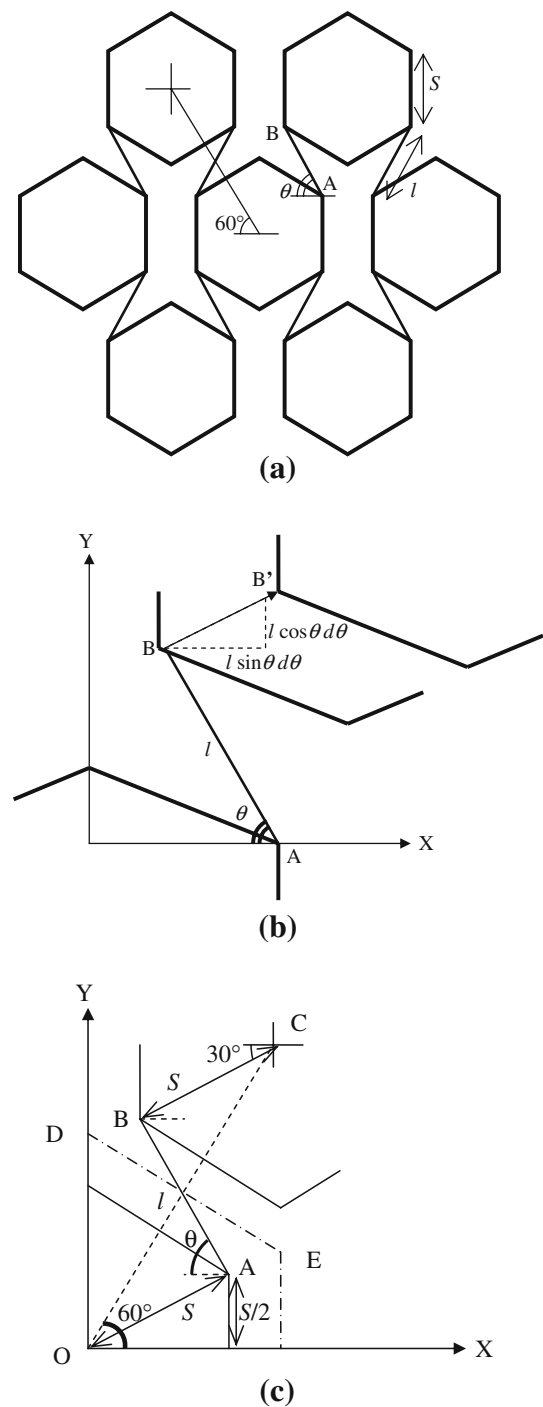


Fig. 2 **a** Hexagonally arranged hexagonal nodules showing fibril length l , hexagonal sides S , and fibril angle θ , **b** displacement of B to B' as a result of clockwise rotation of fibril AB by an angle of $d\theta$, and **c** schematic for the development of 2D Poisson's ratio as a function of density packing factor

by the hexagons to the total area, whereas the 3D density packing factor is calculated as the fraction of the volume enclosed by hexagonal nodules to the total volume.

The boundary DE, which demarcates the empty space between two neighboring hexagons equally, is of the length

$$(\overline{DE}) = 2 \left(S - \frac{l}{\sqrt{3}} \cos \theta \right). \tag{2}$$

From the definition of the 2D density packing factor,

$$d^{(2D)} = \frac{\frac{3\sqrt{3}S^2}{2}}{\frac{3\sqrt{3}(\overline{DE})^2}{2}} = \left[\frac{1}{2} \left(1 - \frac{l}{\sqrt{3}S} \cos \theta \right)^{-1} \right]^2, \tag{3}$$

which is to be related to the Poisson’s ratio

$$v_{xy} = -\frac{\varepsilon_y}{\varepsilon_x}. \tag{4}$$

The displacement of C with respect to O, being equal to that of B with respect to A, can be obtained by a prescription of AB rotation by a clockwise change in angle of $d\theta$ as shown in Fig. 1b to give

$$\begin{Bmatrix} d(\overline{OC})_x \\ d(\overline{OC})_y \end{Bmatrix} = l d\theta \begin{Bmatrix} \sin \theta \\ \cos \theta \end{Bmatrix} \tag{5}$$

and the strains

$$\begin{Bmatrix} \varepsilon_x \\ \varepsilon_y \end{Bmatrix} = l d\theta \begin{Bmatrix} \sin \theta (\sqrt{3}S - l \cos \theta)^{-1} \\ \cos \theta (S + l \sin \theta)^{-1} \end{Bmatrix}. \tag{6}$$

Constraints are (a) rigid hexagonal nodules that displace through curvilinear motion, and (b) rotation of rigid fibril by rotation about the hinging points A and B.

Since

$$\frac{(\overline{OC})_y}{(\overline{OC})_x} = \sqrt{3} \tag{7}$$

for a hexagonal array, we have the relation

$$\frac{l}{S} = \frac{2}{\sin \theta + \sqrt{3} \cos \theta} \tag{8}$$

which leads to

$$\tan \theta = \frac{4\sqrt{d^{(2D)}}}{\sqrt{3}(2\sqrt{d^{(2D)}} - 1)} - \sqrt{3} \tag{9}$$

and

$$v_{xy} = v^{(2D)} = -\frac{1}{\sqrt{3} \tan \theta}. \tag{10}$$

Therefore, the Poisson’s ratios can be expressed in terms of the density packing factor as

$$v^{(2D)} = \frac{1 - 2\sqrt{d^{(2D)}}}{3 - 2\sqrt{d^{(2D)}}} \tag{11}$$

with auxetic characteristics for $0.25 < d^{(2D)} \leq 1$. By analogy, 2D shapes such as squares and circles in comparison to their 3D counterpart, i.e., cubes and spheres, respectively, one has

$$\begin{bmatrix} d_{\text{square}}^{(2D)} & d_{\text{circle}}^{(2D)} \\ d_{\text{cube}}^{(3D)} & d_{\text{sphere}}^{(3D)} \end{bmatrix} = \begin{bmatrix} (x_1/x_2)^2 & (r_1/r_2)^2 \\ (x_1/x_2)^3 & (r_1/r_2)^3 \end{bmatrix}, \tag{12}$$

where x and r refer to the length dimensions and radii, respectively, with subscripts 1 and 2 denote node and representative volume element, respectively, then the density packing factor of a 3D hexagon-like node can be inferred by raising the power to give

$$d^{(3D)} = \left[\frac{1}{2} \left(1 - \frac{l}{\sqrt{3}S} \cos \theta \right)^{-1} \right]^3. \tag{13}$$

It follows that

$$v^{(3D)} = \frac{1 - 2 \times \sqrt[3]{d^{(3D)}}}{3 - 2 \times \sqrt[3]{d^{(3D)}}}, \tag{14}$$

which exhibits auxetic behavior when $0.125 < d^{(3D)} \leq 1$.

To provide a schematic view on the Poisson’s ratios of hexagonal nodules as a function of density packing factor, plots of v versus d were plotted in Fig. 3 based on Eqs. 11 and 14 to represent the 2D and 3D models, respectively. Based on the geometry specified in Fig. 2, the Poisson’s ratio ranges from $v = 1/3$ at $d = 0$ to $v = -1$ at $d = 1$, whereby the 3D model possesses lower Poisson’s ratio compared to that of 2D model for $0 < d < 1$. Although one may expect that the Poisson’s ratio will differ for geometries other than that shown in Fig. 2 (such as skewed hexagonal array and/or skewed hexagonal blocks), one may still expect the Poisson’s ratio based on 3D model will always be lower than that of the 2D model for $0 < d < 1$ except at $d = 0$ and $d = 1$ where the Poisson’s ratios are equal for both models. Based on the geometry specified in Fig. 2, it is possible to convert the Poisson’s ratio of a 2D model to that of a 3D model or vice versa directly by virtue of Eqs. 11 and 14, i.e.,

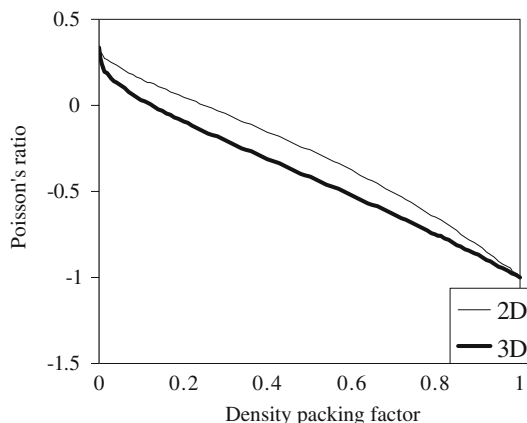


Fig. 3 Comparison between the 2D and 3D models for the Poisson’s ratio of hexagonal blocks in hexagonal array for varying density packing factor

$$\frac{\nu^{(3D)}}{\nu^{(2D)}} = \left(\frac{1 - 2 \times \sqrt[3]{d}}{1 - 2 \times \sqrt[2]{d}} \right) \left(\frac{3 - 2 \times \sqrt[3]{d}}{3 - 2 \times \sqrt[2]{d}} \right) \quad (15)$$

or in the simplified form as

$$\frac{\nu^{(3D)} - \frac{1}{3}}{\nu^{(2D)} - \frac{1}{3}} = d^{-\frac{1}{6}} \left(\frac{3 - 2 \times \sqrt[2]{d}}{3 - 2 \times \sqrt[3]{d}} \right) \quad (16)$$

The Poisson's ratio of nodule-fibril microporous auxetic materials has been developed herein using hexagonal blocks arranged in hexagonal array. The hexagonal shape was selected due to its better approximation to the spherical-like nodules than rectangular blocks. It has been illustrated that with all other conditions fixed, the Poisson's ratio of such a structure in 3D is more negative than an equivalent in 2D. In this article, the hexagonal array is balanced, i.e., the distances between a hexagonal centroid to its six neighboring centroids are equal. As such the present hexagonal model may possess improved accuracy compared to the rectangular model that is arranged in the same hexagonal array. However, the present model lacks the flexibility of the arrangement geometry of the rectangular model [10, 11] which can be achieved by biased hexagonal array with distorted hexagonal nodules. The influence of biased hexagonal array and distorted hexagonal blocks can be investigated in future, in particular addressing the effect of nodule distortion and nodule rearrangement resulting from the extrusion process [12, 13].

Strain-dependent behavior can be obtained by taking integral of Eq. 5 and that the subtended angle between the diagonally neighboring nodes with the horizontal axis is no longer fixed at 60°. The in-plane Young's modulus can be

obtained by incorporating rotational stiffness at the hinging point. The shear moduli can then be obtained from the Young's modulus and the Poisson's ratio. The present model can be extended to incorporate alternative modes of deformation by incorporating a spring stiffness constant to the fibril in order to account for fibril stretching and buckling.

References

1. Lakes RS (1987) *Science* 235:1038
2. Friis EA, Lakes RS, Park JB (1988) *J Mater Sci* 23:4406. doi:[10.1007/BF00551939](https://doi.org/10.1007/BF00551939)
3. Caddock BD, Evans KE (1989) *J Phys D Appl Phys* 22:1877
4. Evans KE, Caddock BD (1989) *J Phys D Appl Phys* 22:1883
5. Yeganeh-Haeri A, Wiedner DJ, Parise JB (1992) *Science* 257:650
6. Keskar NR, Chelikowsky JR (1992) *Nature* 358:222
7. Gibson LJ, Ashby MF, Schajer GS, Robertson CI (1982) *Proc R Soc Lond A* 382:25
8. Hirotsu S (1991) *J Chem Phys* 94:3949
9. Herakovich CT (1991) *J Compos Mater* 18:447
10. Alderson A, Evans KE (1995) *J Mater Sci* 30:3319. doi:[10.1007/BF00349875](https://doi.org/10.1007/BF00349875)
11. Alderson A, Evans KE (1997) *J Mater Sci* 32:2797. doi:[10.1023/A:1018660130501](https://doi.org/10.1023/A:1018660130501)
12. Alderson KL, Alderson A, Davies PJ, Smart G, Ravirala N, Simkins G (2007) *J Mater Sci* 42:7991. doi:[10.1007/s10853-006-1325-8](https://doi.org/10.1007/s10853-006-1325-8)
13. Alderson KL, Weber RS, Evans KE (2007) *Phys Status Solidi B* 244:828
14. Ravirala N, Alderson A, Alderson KL (2007) *J Mater Sci* 42:7433. doi:[10.1007/s10853-007-1583-0](https://doi.org/10.1007/s10853-007-1583-0)
15. Masters IG, Evans KE (1996) *Compos Struct* 35:403